

Electron-spin-resonance studies of the Ag-, Eu-, and Gd-doped Y-Ba-Cu-O high- T_c superconductors

Juh Tzeng Lue

Department of Physics, National Tsing Hua University, Hsinchu, Taiwan, Republic of China

(Received 22 March 1988; revised manuscript received 1 June 1988)

The electron-spin resonance (ESR) of pure and Ag-, Eu-, and Gd-doped $\text{YBa}_2\text{Cu}_3\text{O}_{7-\delta}$ are measured at temperatures above and below the transition temperature T_c . The ESR signals are speculated to be due to electrons in the $d_{x^2-y^2}$ levels of the Cu^{2+} ions hybridized with the oxygen $2p$ electrons in the tetragonal CuO_4^{2+} structure above the quasi Fermi level which lies at the middle of the Mott-Hubbard gap. For the pure orthorhombic structure or properly doped impure structures, the ESR signals disappear even at $T > T_c$, implying a net spin $S=0$ due to the superexchange force of the Cu^{2+} ions through the intermediate oxygen atoms.

The bonding characteristic of the Cu-O bond in the high- T_c Y-Ba-Cu-O systems plays an important role in the superconducting mechanism. The degenerate $|d_{z^2}\rangle$ and $|d_{x^2-y^2}\rangle$ states of the E_g orbitals in the CuO_6 octahedra are split into two Kramers doublets by the lower symmetry of the orthorhombic and tetragonal structures. The spin-orbit interaction $\lambda\hat{L}\cdot\hat{s}$ can admix the ground states into the excited states and yield an anisotropic g value given by¹

$$g_{\parallel} = 2 \left[1 + \frac{4\lambda}{\Delta_0} \right], \quad g_{\perp} = 2 \left[1 + \frac{\lambda}{\Delta_1} \right], \quad (1)$$

where Δ_0 and Δ_1 are the energy difference between the ground $|x^2-y^2\rangle$ and the excited $|xy\rangle$ and $|yz\rangle$, $|zx\rangle$ states, respectively. Since the linewidth of the ESR signals is much broader than those from the paramagnetic Cu^{2+} ions, we may speculate that the resonance comes from the hybridization of the $|d_{x^2-y^2}\rangle$ orbits of the Cu^{2+} ions with the p electrons of oxygen in the tetragonal structure into the conduction band which lies in the middle of the Hubbard gap.²

The spins of Cu^{2+} ions can interact with the lattice or with spins of neighboring Cu^{2+} ions by the superexchange force. The Hamiltonian can be written as

$$H = V_{e,l} + H_h - \sum_j V_j Q_j - t \sum_{i,j} C_{i\sigma}^\dagger C_{j\sigma} + U \sum_i n_{i\uparrow} n_{i\downarrow}, \quad (2)$$

where the V_j 's are electronic operators,³ Q_j are the normal phonon coordinates, t is the effective one-electron transfer integral, U is the on-site repulsive energy, $C_{i\sigma}$ is the fermion operator, and $n_{i\sigma} = C_{i\sigma}^\dagger C_{i\sigma}$ is the number operator for electrons of spin σ at site i . The superexchange interaction $J = 2t^2/U$ is about 0.0625 eV for the quaternary compound $(\text{Y}_{1-x}\text{Ba}_x)_2\text{CuO}_{4-y}$.⁴ For a half-filled band in the singly occupied site subspace, the Hamiltonian can be simplified to $H = J \sum_{i,j} (\mathbf{S}_i \cdot \mathbf{S}_j - \frac{1}{4})$. The superexchange interaction J is enhanced by the vibronic (vibrational-electronic) field effect arising from the distorted Cu-O plane in the orthorhombic structure.⁵ This can be realized when the CuO_2 square planar layer is bent down or up, the distance between the Cu and O atoms

becoming closer and the convalency behavior increasing, resulting in an increase of the $d-p$ hybridization. The spins of two neighboring Cu^{2+} ions with $S = \frac{1}{2}$ for each ion, can interact by J through the intermediate O atoms to form a singlet pair with $S=0$. As Williams, Krupka, and Breen⁶ and Lee and Walsh⁷ pointed out in early 1968, the tunneling matrix elements between the vibronic wave functions of the distorted configurations may occur more rapidly between states of opposite spins than between the Kramers conjugate states and provide a plausible mechanism for an enhanced exchange force. If the ESR probing frequency ν is much smaller than the exchange frequency J/h ($\sim 1.5 \times 10^{13}$ Hz), then one would detect a diamagnetic state (actually it is an antiferromagnetic state with very fast exchange of spin up and down between the neighboring Cu^{2+} ions), and no ESR signal can be observed in the pure orthorhombic $\text{YBa}_2\text{Cu}_3\text{O}_{7-\delta}$ structure.

With the existence of oxygen deficiency in the Cu-O bond, the superexchange force J becomes weaker, and it is possible to observe local moments at each copper ion. Since the dipole-dipole interaction between neighboring Cu^{2+} ions is still high enough to overwhelm the hyperfine interactions of the impurity-doped samples, the ESR linewidth is very broad and exhibits a single line.

To perform the experiments, the samples were prepared by solid-state reaction using 99.9% pure Y_2O_3 , BaCO_3 , CuO , and doping oxides. The weighted mixture was mixed in ethanol on a hot plate stirred magnetically until dry. The powder was calcined at 900°C in air for 12 h, then finely ground and washed in acetone and finally pressed in a proper pellet for further sintering. The pellets were sintered at 950°C in oxygen for 16 h and then furnace cooled. The crystal structure was examined by x-ray diffraction analysis (XRDA).

The ESR spectra were measured by employing a Bruker GmbH-type ER-200 spectrometer with a TE₁₀₄ double rectangular cavity at a modulating frequency of 100 kc/s. Figure 1 shows the ESR signals of the sample (1a), $\text{Y}_{1.5}\text{Ba}_{0.5}\text{Cu}_3\text{O}_9$ without a superconducting phase, and the sample (1b), $\text{Y}_1\text{Ba}_2\text{Cu}_3\text{O}_{7-\delta}$ with $T_c = 90$ K. Wings exist at the lower-field side of the signal as shown with sample (1b). When the sample is vacuum annealed at 500°C for 1 h, the signal as shown with sample (1b) loses the wings

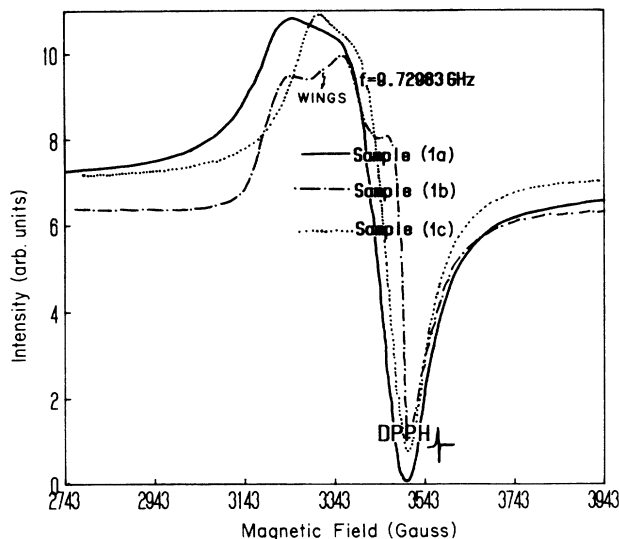


FIG. 1. ESR signals measured at room temperature for sample (1a), $Y_{1.5}Ba_{0.5}Cu_3O_9$ (nonsuperconducting), sample (1b), $Y_1Ba_2Cu_3O_{7-\delta}$ ($T_c = 90K$), and sample (1c), sample (1b) vacuum annealed.

and becomes similar to sample (1a). As the temperature is cooled down to 77 K, the ESR signal of sample (1a) is unchanged [as plotted in Fig. 2a], whereas the whole signal of sample (1b) greatly diminishes [as shown in Fig. 2(b)], which implies an unusual repelling force to the recorder at the onset of the magnetic sweep, a force resulting from the Meissner effect. If sample (1b) is ground to powder, the ESR signals almost keep the same intensities whether the temperatures are at 300 or 77 K, implying that the signal may come from the nonsuperconducting state and that the diminishing of the ESR signal in Fig. 2(b) is due to the narrowing of the penetration depth of the magnetic field in the superconducting states.

For pressure-sintered samples for which the critical current density J_c can be enhanced to higher than 500

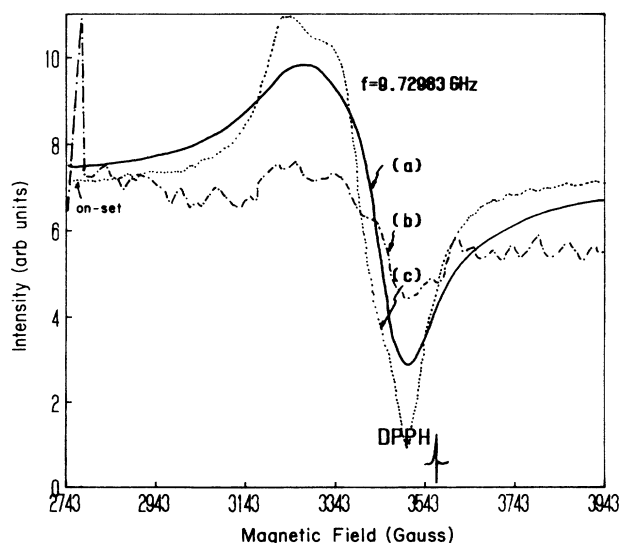


FIG. 2. ESR signals measured at 77 K for (a) sample (1a), (b) sample (1b), and (c) powder of sample (1b).

A/cm², the ESR signal vanishes as shown in Fig. 3 for sample (3a). When this sample is ground to powder, the base line for sample (3b) as shown in Fig. 3 shifts with the magnetic field as a result of the rf absorption arising from the nonzero magnetic susceptibility within the broadened spin-spin states. We suppose that the superexchange force which yields $S=0$ in the pure orthorhombic structure is a volume property and will be weakened as the particle size is reduced. This is clearly revealed by the fact that a non-superconducting layer intrinsically exists on the surface of the high- T_c superconductors as detected in Josephson tunneling experiments.^{8,9} If this good sample is vacuum annealed at 600°C for 1 h, an ESR signal similar to sample (1a) appears, as shown in Fig. 3 for sample (3c). The oxygen deficiency induces a transition from orthorhombic to tetragonal structure, implying a nonsuperconducting phase. The experimental results exclude the possibility that the ESR can only come from the green-phase 2:1:1 compound as proposed by Bowden *et al.*¹⁰

The ESR spectra of the Ag interstitially [sample (4a) in Fig. 4] and Gd substitutionally [sample (4b) in Fig. 4] doped $Y_1Ba_2Cu_3O_{7-\delta}$ are not very different from the undoped sample [sample (1b) in Fig. 1], except that the linewidth is a little sharper in the doped samples. Since the Ag atoms are found interstitially doped, we may expect that the ESR comes from the Cu ions. A peculiar result is the vanishing of the ESR signals for the Eu substitutionally doped [sample (4c) in Fig. 4] and the Ag interstitially doped samples (with $AgNO_3$ as the dopant) at a concentration around 0.25 wt.%. The XRD analysis as shown in Fig. 5 reveals a sharp increase of the b axis and a sharp drop of the c axis at this doping level. Also, the x-ray diffraction patterns indicate a preferable crystal orientation and the critical current density is enhanced 15-fold at this doping concentration. When the samples are stored in air for several weeks, the Ag-doped sample completely loses its superconductivity and the ESR spectrum

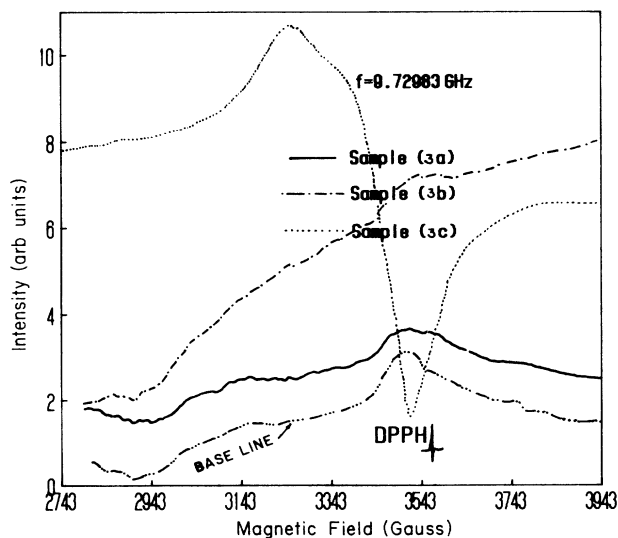


FIG. 3. ESR signals measured at 300 K for sample (3a), pressure-sintered sample with high J_c , sample (3b), powder of sample (3a), and sample (3c), vacuum annealed at 600°C for 1 h.

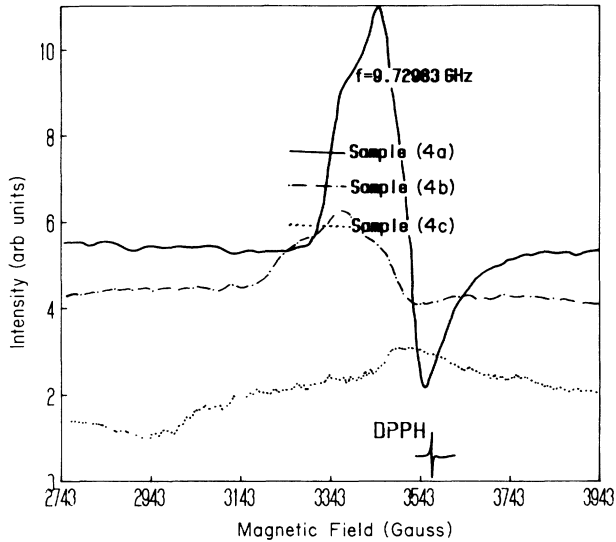


FIG. 4. ESR signals measured at 300 K for (a) Ag (2 wt.%) interstitially doped $\text{YBa}_2\text{Cu}_3\text{O}_{7-\delta}$ ($T_c = 93$ K), (b) Gd, $\text{Gd}_2\text{Cu}_3\text{O}_{7-\delta}$ ($T_c = 91.4$ K), and (c) $\text{Eu}_1\text{Ba}_2\text{Cu}_3\text{O}_{7-\delta}$ ($T_c = 94.5$ K).

becomes split since the spin-lattice relaxation rate is proportional to the square of the spin-orbit interaction constant, which is much larger for copper ions than for Ag atoms. The hyperfine lines of Cu^{2+} become broadened and tend to yield a single line. We may expect that the hyperfine lines as shown in Fig. 6(a) arise from Ag ions and that the absorbed water may catastrophically weaken the dipole-dipole interaction. The ESR of sample (1b) stored in air in the same condition is also plotted in Fig. 6(b) for comparison.

The chemical shifts of the core electrons of the Y-Ba-Cu-O system as measured by a Perkin Elmer PHI 1905 spectrometer indicate that the line shape and core binding energies of $\text{Ag}(3d_{5/2})$ and $\text{Ag}(3d_{3/2})$ are the same as those in the pure bulk Ag, assuming that the doped Ag atoms are in the interstitial sites. The core binding energy spectra of $\text{Cu}(2p_{3/2})$ and $2p_{1/2}$ as shown in Fig. 7 imply the presence of shake-up lines in the Ag-doped

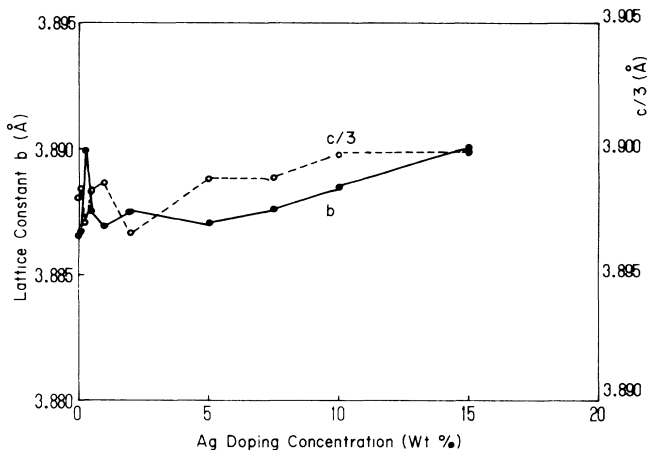


FIG. 5. The change of the lattice constants b and c vs Ag doping concentration as measured by XRD.

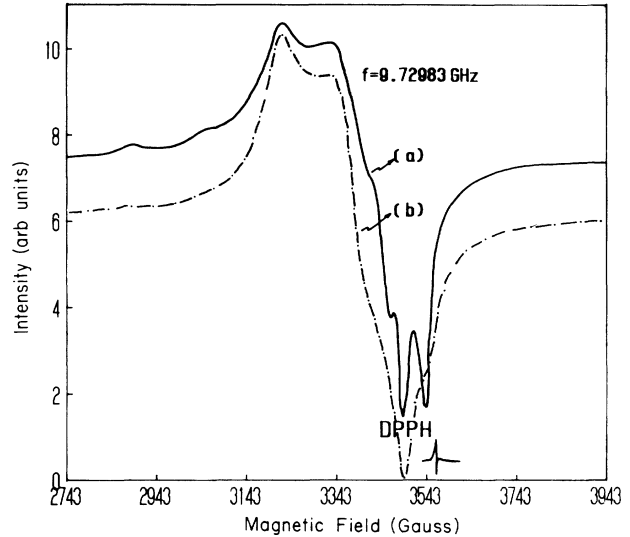


FIG. 6. ESR of (a) the Ag-doped (3 wt.%) $\text{Y}_1\text{Ba}_2\text{Cu}_3\text{O}_{7-\delta}$, and (b) the undoped sample (1b), stored in air for 6 weeks.

$\text{YBa}_2\text{Cu}_3\text{O}_{7-\delta}$ compound. These shake-up lines usually arise from the monopole transition in the paramagnetic states of the copper ions.¹¹ The absence of the shake-up satellites in the undoped samples is usually characterized by the elemental or diamagnetic states. Since both diamagnetic and paramagnetic samples are superconductors, it is difficult to understand the origin of the superconducting states from the view point of a magnetic state at T above T_c . However, the possible enhancing of the superexchange force J by Ag doping may help to condense the conduction electrons near the Fermi level to form Cooper pairs as the temperature decreases below T_c .

The origin of the ESR signal is supposed to be due to the $d_{x^2-y^2}$ electrons of Cu^{2+} ions hybridized with the oxygen p electrons into the conduction band through the superexchange force J . In a pure orthorhombic structure, J is strong enough to insure $S=0$ for the neighboring copper ions. In the presence of a tetragonal structure due

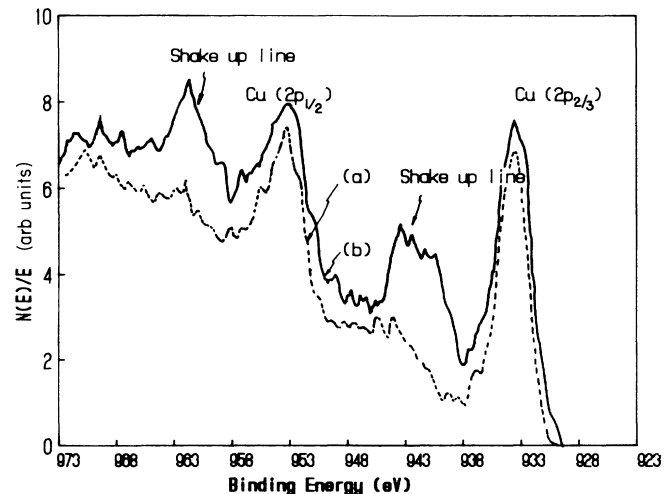


FIG. 7. Core binding energy spectra of Cu for (a) the undoped, and (b) Ag 0.1% doped $\text{YBa}_2\text{Cu}_3\text{O}_{7-\delta}$ compound.

to oxygen deficiency, J is weakened enough to result in local moments. If the oxygen-deficiency density is not high, these spin-up and spin-down electrons in neighboring Cu^{2+} ions can experience collective motion, giving rise to spin waves while still becoming superconductive. In increasing the oxygen deficiency further, the collective motion is interrupted and the sample becomes insulating. The dipole-dipole interaction is still large enough to broaden the ESR lines although the compounds are insulating with a line shape almost the same as in the conducting state. The ESR signal coming from the conduction electrons (or holes in valence band) in the superconducting states with an impurity phase can be explained as follows.

(1) For ionic local moments, the magnetic susceptibility would exhibit a Curie temperature dependence. But the nearly constant variation of the susceptibility above T_c clearly reveals that it is due to Pauli antiferromagnetism arising from conduction electrons.

(2) The line shape is not a simple Dysonian deduced intrinsically from the rf absorption of conduction electrons in metals, but rather comes from composite lines at different sites. Moreover, the linewidth of the paramagnetic Cu^{2+} spin resonance would be more narrow and symmetric.^{12,13}

(3) The carrier relaxation time τ is related to the spin-lattice relaxation time τ_1 by¹⁴

$$\tau \approx (\Delta g)^2 \tau_1, \quad (3)$$

where Δg is the g shift from free electrons and τ_1 , in the normal skin effect, is related to the linewidth ΔH by^{15,16}

$$\tau_1 \approx \frac{1.12}{r_e \Delta H}, \quad (4)$$

where r_e is the electron gyromagnetic ratio. The calculated $\tau \approx 3.2 \times 10^{-10}$ sec combined with the carrier density ($n \approx 10^{22} \text{ cm}^{-3}$) as estimated by Mattheis¹⁷ would imply a resistivity of 0.65 m Ω cm, which is comparable to the values of the resistivity measured at room temperature. The fairly ESR-independent linewidth with respect to temperature may be due to the spin-phonon interaction in the Cu-O (110) plane being very weak. The ESR signals are possibly due to electrons in the $d_{x^2-y^2}$ levels of the

Cu^{2+} ions hybridizing with the oxygen $2p$ electrons in the tetragonal CuO_x^{2+} structure above the quasi Fermi level, which lies in the middle of the Mott-Hubbard gap. The electrons are localized with zero momentum. Conduction is not by carrier drift but rather by the propagation of electron-spin flip-flop analogous to water waves. The superexchange force J plays an important role in transforming the ceramic from an insulating into a superconducting state.

The wings appearing at the lower side of the spin resonance spectra, which are considered to be antiferromagnetic spin waves,¹⁸ need further verification. The possibility of the signal coming from Cu^{2+} ions in the vicinity of defects and impurities can be excluded, since such signals would have Curie-like temperature dependence. We suspect that these signals come from the reflections of the three g factors associated with Cu in an orthorhombic site, because then the signal will also appear in the green phase. These signals disappear if the samples are vacuum annealed at 500°C for 1 h wherein the impurities still remain. The spin wave will be interrupted when the Cu-O bonds in the conducting (110) planes are broken. The Cu-O bonds usually introduce a B_{3u} stretching vibration mode, occurring at 630 cm^{-1} .¹⁹ Similar spin-wave line shapes have been observed in GeNb (Ref. 20) and permalloy films.²¹ Spin-density-waves instability can introduce an energy gap with a temperature variation analogous to a superconducting gap.²² This long-range force possessed by spin waves existing at temperatures above T_c has a tendency to cause neighboring electrons to form Cooper pairs and induce collective motion. Since the spin-density wave will compete with the superconducting pairing states, the antiferromagnetic spin waves diminish before the material becomes a superconductor and are detected in this experiment. They are also shown in the spectra of Ref. 12.

The author is indebted to Dr. P. T. Wu, Dr. W. H. Lee, Dr. J. H. Kung, Dr. O. Meyer, Mr. H. H. Yen, and Mr. Y. C. Chen for providing the samples and the x-ray analysis. This work was supported by the National Science Council of the Republic of China.

¹B. Bleaney, K. D. Bowers, and M. H. L. Pryce, Proc. R. Soc. London Ser. A **228**, 166 (1955).

²G. Baskaran, Int. J. Mod. Phys. B **1**, 49 (1987).

³C. Y. Huang and J. T. Lue, Prog. Theor. Phys. **43**, 10 (1970).

⁴A. E. Ruckenstein, P. J. Hirschfeld, and J. Appel, Phys. Rev. B **36**, 857, (1987).

⁵H. Kamimura, Int. J. Mod. Phys. B **1**, 225 (1987).

⁶F. I. B. Williams, D. C. Krupka, and D. P. Breen, Phys. Rev. **179**, 255 (1969).

⁷K. P. Lee and D. Walsh, Phys. Lett. **27A**, 17 (1968).

⁸J. S. Tsai, Y. Kubo, and J. Tabuchi, Phys. Rev. Lett. **58**, 1979 (1987).

⁹B. Golding, N. O. Birge, W. H. Haemmerle, R. J. Cava, and E. Rietman, Phys. Rev. B **36**, 5606 (1987).

¹⁰G. J. Bowden *et al.*, J. Phys. C **20**, L545 (1987).

¹¹T. C. Carlson, *Photoelectron and Auger Spectroscopy* (Plenum, New York, 1975), p. 174.

¹²R. Mehran, S. E. Barnes, T. R. McGuire, W. J. Gallagher, R. C. Sandstrom, T. R. Dinger, and D. A. Chance, Phys. Rev. B **36**, 740 (1987).

¹³F. Mehnert, K. W. H. Stevens, M. W. Shafer, and W. J. Fitzpatrick, Phys. Rev. B **32**, 7083 (1985).

¹⁴R. J. Elliott, Phys. Rev. **96**, 266 (1954).

¹⁵G. Feher and A. F. Kip, Phys. Rev. **98**, 337 (1955).

¹⁶J. T. Lue, Nuovo Cimento B **22**, 1 (1974); **26**, 243 (1975).

¹⁷L. F. Mattheis, Phys. Rev. Lett. **58**, 1028 (1987).

¹⁸J. T. Lue and P. T. Wu, Solid State Commun. **66**, 55 (1988).

¹⁹M. Stavola, D. M. Krol, W. Weber, S. A. Sunshine, A. Jayaraman, G. A. Kourouklis, R. J. Cava, and E. A. Rietman, Phys. Rev. B **36**, 850, (1987).

²⁰S. N. Ekbotte, S. K. Gupta, and A. V. Naplikar, Solid State Commun. **36**, 117 (1980).

²¹W. M. Moller and J. Juretschke, Phys. Rev. B **2**, 2651 (1970).

²²A. W. Overhauser, Phys. Rev. **128**, 437 (1962).